Author Version of : Marine Pollution Bulletin, vol.163; 2021; Article no: 111939

Total organic carbon and its role in oxygen utilization in the eastern Arabian Sea

Suhas S. Shetye[1], Siby Kurian[1], Vidya P.J[2], Mangesh Gauns[1], Damodar M. Shenoy[1], Aparna, S. G.[1], Nandakumar K[1], Supriya G. Karapurkar[1]

[1]CSIR-National Institute of Oceanography, Dona Paula- 403 004, Goa, India

[2]National Centre for Polar & Ocean Research, Ministry of earth sciences, Headland Sada, Goa-403 804, India

Abstract:

We report seasonal and temporal variation of total organic carbon (TOC) in the eastern Arabian Sea (AS). In comparison to the deep, TOC in the top 100 m showed spatial variation with higher concentrations towards northern AS during North east monsoon (NEM) and South west monsoon (SWM). A comparison with the US-JGOFS data (1995) shows warmer temperatures, enhanced TOC and low chlorophyll in the recent years. High TOC is associated with Arabian Sea high saline waters (ASHSW), advected from the Arabian Gulf, might have resulted in an enhancement of TOC in the eastern AS. This excess TOC supports a high abundance of bacteria despite the low primary productivity. TOC oxidation accounted for 14.3% and 22.5% of oxygen consumption for waters with potential density between 24.5 to 27.3 kg/m^3. This study attains great significance considering the missing links with respect to the role of transport processes in ocean deoxygenation under ongoing warming scenarios.

Keywords: Organic carbon, oxygen minimum zone, Arabian Sea, phytoplankton, apparent oxygen utilization.

Introduction:

Dissolved oxygen (DO) is the basic necessity for life in oceanic waters and changes in DO can greatly affect marine biodiversity. Large areas in the ocean, especially in the tropics, houses oxygen minimum zones (OMZ) at intermediate depths (Stramma et al., 2008). The estimated volume of OMZs with DO concentrations < 20 μmol/kg is only about 1% and < 5 μmol/kg is about 0.05% of the global ocean volume (Lam and Kuypers, 2011). The recent modelling studies indicate a significant decrease in the DO levels over the next few decades (Bopp et al., 2013; Cocco et al., 2013), with possible expansion and intensification of tropical OMZs (Codispoti, 2010). Recently, Schmidtko et al. (2017) have shown that global oceanic DO content of 227.4 ± 1.1 petamoles (10^{15} mol) has decreased by more than 2% (4.8 ± 2.1 petamoles) since 1960. (Many other studies also report decreasing levels of DO and expansion of OMZs worldwide (Stramma et al., 2008; Keeling et al., 2010; Breitburg et al., 2018; Lachkar et al., 2019), thus making it vital to study oceanic regions with OMZ.

In the world oceans, one of the most intense OMZ lies in subsurface waters of the AS, and other regions include the areas of the eastern boundary upwelling (EBU) regions in the tropical oceans off California, Peru, and Namibia (Naqvi et al., 2006; Karstensen et al., 2008). The Persian Gulf water (PGW) spreads over large parts of the AS with its core identified by a salinity maximum centered around 26.6 σ_θ (Wyrtki, 1971; Prasad et al., 2001). This density level corresponds to the core of the intense OMZ of the AS where denitrification is at its maximum (Deuser et al., 1978; Naqvi, 1987; Codispoti et al., 2001; Ward et al., 2009). Various researchers have studied the changes in the dissolved oxygen concentrations in the AS. Recently, Shenoy et al. (2020) showed that the westward propagating Rossby waves from the west coast of India strongly influence the AS OMZ by modulating the flow of Indian Central Water (ICW) into the OMZ. Previously, Banse et al. (2014) used more than four decades of DO measurements from the AS OMZ and reported marked seasonality, with elevated DO levels during the NEM and spring inter-monsoon (SIM) as compared to the SWM. They also observed a significant decline in the DO concentrations between 12°N and 20°N.

DO concentrations are regulated by the oxygen produced via primary production, loss via respiration, ventilation through the atmospheric exchange and advection by currents. Warming is considered as a major driver for deoxygenation through its effects on solubility, circulation, mixing and oxygen respiration (Oschlies et al., 2018). Roxy et al. (2014) showed that the western tropical Indian Ocean is warming faster than the rest of the tropical oceans. Recently, Sun et al. (2019) showed that the warming rate of the AS has significantly increased during the past two decades.

Dinesh Kumar et al. (2016) reported the rate of sea surface temperature (SST) increase as 0.12°C per decade in the AS for the period from 1960 to 2009. Such warming can affect the solubility of gases in the AS. Although the solubility effects have been quantified (Oschlies et al., 2018), contributions from other mechanisms such as transport processes and respiratory oxygen demand are still not fully understood.

Total organic carbon (TOC) plays a vital role in the consumption of oxygen, leading to the formation of OMZ. Recently, Al-Said et al. (2018) reported very high TOC concentrations (318.4 μM) due to anthropogenic activities in the Kuwaiti waters as compared to Kuwaiti offshore waters (mean 130.8 μM). They also suggested that the high-salinity water mass that flows out of the Gulf has high TOC concentrations and may cause expansion/intensification of the AS OMZ. However despite playing an important role in the sustenance of AS OMZ, very few studies have been carried out on the TOC in the AS. The latest TOC study in the AS dates back to the 1990's report of US-JGOFS (Hansell and Peltzer 1998). They reported maximum mixed-layer TOC concentrations of 80–95 μM during NEM. Prior to that, dissolved organic carbon (DOC) concentrations of 0.6 to 0.89 mg/L were reported in the euphotic zone of the northern AS (Menzel 1964). Later Kumar et al. (1990) also studied TOC in the AS, however, the exceptionally high concentrations presented by them were not reported from any other open ocean waters. In this study, we investigate the spatio-temporal variations of TOC in the eastern AS, comparison with earlier data, and estimate the contribution of TOC oxidation to oxygen consumption.

1.1 Circulation in Arabian Sea:

Seasonal reversal of monsoonal winds, from the southwest during the summer and from the northeast during the winter, makes the AS a unique region. During the winter monsoon (November - February), cold and dry northeast monsoon winds causing evaporative cooling in the northern part of the AS (Dickey et al., 1998), which further causes deepening of the mixed layer and upward entrainment of nutrients into the surface layers and leads to a winter bloom (Banse, 1987; Madhupratap et al., 1996). During summer monsoon (June - September), the low-level Findlater jet (Findlater, 1969), causes strong upwelling of cold and nutrient-rich subsurface water along the coast of Somalia and Oman (Schott and McCreary, 2001) and leads to phytoplankton bloom (Banse, 1987). Apart from these, the region is influenced by the three types of high-salinity water masses: the Arabian Sea high-salinity water (ASHSW), the Persian Gulf water (PGW), and the Red Sea water (RSW) (Rochford 1964; Morrison 1997). The ASHSW originate in the northern AS through deep convective mixing during winter (Han et al., 2001), and spreads to the southern part as salinity maximum within the upper 150 m (Kumar and Prasad 1996; 1999). The PGW forms in the Persian

Gulf and spreads over the AS with its core identified by a salinity maximum (26.6 kgm^{-3}) at 250-300 m (Wyrtki, 1971; Prasad et al., 2001). The Red Sea water forms in the Red Sea and spreads to the Arabian Sea as a high saline intermediate water with the core centred around 27.2 kgm^{-3} as σ_θ at 500-700 m (Beal et al., 2000). Using Argo float data, Joseph and Freeland (2005) studied the temporal and spatial variations of the ASHSW. More recently, Zhang et al. (2020) showed enhanced spreading of the ASHSW and PGW from the Gulf of Oman to the northern AS during the recent periods (2014 - 2017). The criteria for identifying the watermasses in the present study is given in table 1.

Table 1: Thermohaline characteristics and core depth of the three high salinity water masses in the Arabian Sea (Prasanna kumar and Prasad 1999)

Water mass	Temperature (^{0}C)	Salinity	σ_θ	Depth (m)
ASHSW	24 - 28	35.3 – 36.7	22.8 - 24.5	0 – 100
PGW	13 - 19	35.1 – 37.9	26.2 - 26.8	200 - 400
RSW	9 - 11	35.1 – 35.7	27.0 - 27.4	500 - 800

2. Material and Methods:

2.1 Sample collection

Water column measurements were carried out under the INDIAS_IDEA programme (funded by CSIR) along a meridional transect at 68°E extending from 8°N to 21°N cutting across the AS OMZ during the SWM (September 2016; SSD 26) and NEM (February 2017; SSD 33) seasons. In addition, measurements carried out at the Arabian Sea Time Series station (ASTS; 17°N 68°E; established under SIBER-INDIA programme) during NEM of 2016, SWM of 2017, and SIM of 2015 and 2019 are also used to compare with the US-JGOFS data. Figure 1a & b represent the station locations of present study and US-JGOFS.

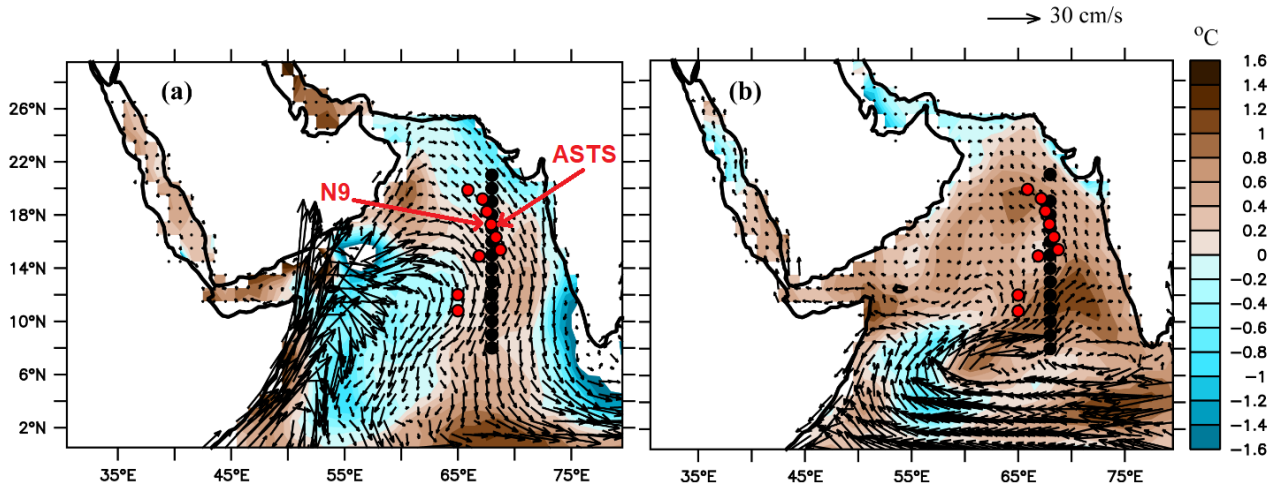

Figure 1: Differences in temperature in the upper 100 m water column during present study versus during US-JGOFS (a) SWM (September 2016 minus September 1995) and (b) NEM (February 2017 minus February 1995). Currents overlay the differences in temperatures. Filled black circles indicate sampling locations of present study and filled red circles represent stations sampled during US-JGOFS.

2.2 Biogeochemical parameters

High-resolution temperature and salinity data were obtained from CTD (SBE 19 plus, Sea Bird Electronics, USA) attached to the rosette. The accuracy of temperature and conductivity for CTD system was ±0.001°C and ±0.0001 S m^{-1}, respectively. The DO samples were fixed and analysed following the Carpenter modification of the Winkler method (Carpenter, 1965). The titration was automated using ODF PC software compiled in LabView, in which the end point is detected photometrically at 365 nm. This methodology gave a precision of 0.1 µM with an accuracy of better than 1%. The detection limit of this automated method was 3 µM. AOU is calculated as AOU = O_2' - O_2, where O_2' is the value of O_2 in the water if it was in equilibrium with the atmosphere. The O_2' values were calculated using the equation of Garcia and Gordon (1992) based on the O_2' values of Benson and Krause (1984). O_2 is the dissolved oxygen measured in the same water sample.

2.3 TOC, TN and POC

Seawater for TOC and total nitrogen (TN) was collected into acid-cleaned 30 mL glass vials and immediately frozen upright at −20 °C. Samples were transferred in −20 °C conditions to the shore laboratory (CSIR-NIO) and analysed within 15 days of its collection. TOC and TN analyses were done using Shimadzu TOC-LCPH analyzer coupled with a TN analyzer. TOC was analyzed at 680°C following combustion catalytic oxidation method (Dickson et al., 2007). TN was analyzed at 720 °C following chemiluminescence method, wherein the nitrogen oxidation product nitric oxide

(NO) is quantified by reaction with ozone and detection of the resulting chemiluminescence (Badr et al., 2003; Letscher et al., 2013). Standardization was achieved using potassium hydrogen phthalate for TOC and potassium nitrate for TN and a 5 point calibration curve was generated before each batch of analyses. To minimize the instrumental blank, conditioning of the combustion tube was performed through repeated injections of Milli-Q water (n=10) prior to analysis of samples. The instrument blank was measured after every five samples using Milli-Q water. Blank concentrations ranged from 90 to 150 µg/L for TOC and 20 to 40 µg/L for TN. All TOC and TN concentrations reported are corrected for the instrument blank. CRM (Deep Sea standard; 41 − 44 µM for TOC and 30.5 - 32.5 µM for TN; batch number 15-2015) procured from University of Miami were run in each batch, and the accuracy of the analysis was ±1 µM. In addition, standards prepared from potassium hydrogen phthalate and potassium nitrate were run during sample analysis. For particulate organic carbon (POC) analysis, water samples (5-10L) were collected in pre-cleaned carboys and vacuum filtered immediately through combusted (@450°C for 5hrs) GF/F filter papers. Filter papers were then stored in sterile single packed petri dishes at -20°C until the analysis. The filters were acid (HCl) fumigated and dried aliquots of filter paper were packed in tin capsules before being combusted in Elemental Analyser (EA) (Flash 1112 make Thermo). Thermal conductivity detector (TCD) was used to determine the POC. Acetanilide and Atropina standards were used to calibrate the TCD of the EA. The precision of our analysis was better than ±2% (for ±1σ).

2.4 Chlorophyll *a* analysis

For the chlorophyll *a* analysis, 1 L of water sample was immediately filtered using a GF/F filter (0.7 µm; 25mm) avoiding exposure to direct light and preserved at −80°C until analysis. The frozen filters were extracted with 100% methanol and analyzed using high performance liquid chromatography (Agilent Technologies) using an Eclipse XDB C8 column following the modified method of Van Heukelem (2002) as described in Kurian et al. (2012). Calibration standards were procured from DHI, Denmark.

2.5 Total bacterial count analysis

Subsamples (20–50 ml) for total bacterial count (TBC) were fixed with 4% of 0.22 µm filtered formaldehyde and stored in the dark at 4°C following the JGOFS Protocols (UNESCO, 1994). These samples were later filtered on black polycarbonate filters (0.2 µm, Nucleopore) and DAPI stained direct counts (AODC) were made. Counting was done using a 100xoil immersion objective of Olympus BH2 epifluorescence microscope (Olympus Corp., Tokyo, Japan). Up to 25 microscopic

fields were counted and averaged counts per field were calculated, and the number of bacterial cells per litre was determined following Parsons et al. (1984).

2.6 Source of satellite data

The monthly mean ocean parameters such as temperature, salinity and currents with spatial resolution 1 x 1 degree for the period 1994 January to 2017 December is acquired from European Centre for Medium-Range Weather Forecasts (ECMWF) Ocean Reanalysis System 4 (ORAS4) (Balmaseda et al., 2013); http://www.ecmwf.int/products/forecasts/d/charts/oras4/reanalysis/. Time series of anomalies of temperature and salinity are calculated by removing the climatological monthly means from the actual data.

2.7 Regression analysis

In the present study the variables AOU and TOC are both dependent on oceanic conditions. Hence we used Model 2 linear regression (Major axis) defined by Karl Pearson (1901). The mathematical derivations are given in York (1966). The matlab or octave code for the same is available at https://www.mbari.org.

3. Results

Here we try to understand the seasonal and spatial variation of TOC in the AS, as it is critical for the sustenance of OMZ in the AS and in the emission of carbon dioxide. The spatial anomalies of temperature in the upper 100 m water column from the JGOFS time to the recent years during SWM and NEM are shown in Fig. 1a and 1b, respectively. Consistent with the measured values, temperature did not show much difference (~ -0.2^{o}C) in the northern stations while it showed a ~0.4-0.5^{o}C increase in the southern region during SWM (Fig. 1a). But during NEM, temperature showed ~0.6-0.7^{o}C increase in the northern part whereas an increase of 1.2 ^{o}C was noted in the southern stations (Fig 1b). The vertical distribution of temperature and salinity are shown in section 3.2. Oxygen distribution in the upper 1000-m water column varied between undetectable and 4.63ml/L (Fig. S1). In the upper 50 m layer, the DO concentrations were >4 ml/L. In general, the oxycline was around 150-m depth, below which the oxygen concentration was <1ml/L. The DO distribution in the top 150-m layer during the NEM was different compared to that in the SWM, with clear signatures of oxycline deepening (up to 180 m) between 19 and 21°NDuring SWM, the southern boundary of OMZ was located around 10°N at ~200 m.

3.1 Seasonal variation of biogeochemical parameters

TOC in the surface waters exhibited a clear spatial pattern with higher concentrations towards the north (Fig. 2a &b). The seasonal variability was less pronounced in the southern stations (8 to 14°N). However, the mean TOC concentration was high during SWM as compared to NEM. The concentrations of TOC in the surface layer varied from 69-148 μM (SWM), and 75-94 μM (NEM). Average TOC in the top 100 m water column was 81μM (SWM) and 78μM (NEM). Recently, Panagiotopoulos et al. (2019) reported that dissolved organic carbon concentrations in the southwest Pacific ranged from 47 to 81μM (0–200 m water column). During SWM, TOC concentrations were high throughout the transect with maximum concentration at the northern stations. Although the average TOC was low during NEM, it was high in the northern stations. In deeper waters (>1000m) TOC was 42.4±1.78 μM and 42.5±2.9 μM during SWM and NEM respectively (Fig 2 c & d).

TBC was high during SWM compared to NEM with higher values towards the north with counts reaching up to 0.85 $x10^9$/L at 16°N (Fig. 2e). Higher concentrations were found at ASTS during NEM reaching 0.74 $x10^9$/L (Fig. 2f). On the contrary, Chl*a* was high during NEM as compared to SWM (Fig. 2g & h). During SWM, Chl*a* showed intense subsurface maxima at 60-70 m depth, except at the northern station (II-14) (Fig. 2g). However, during NEM Chl*a* showed higher values in the upper 100m in the northern stations (from 15ºN onwards; Fig. 2h). The concentration of TN did not show much variations during SWM and NEM with low concentrations in the southern stations. In contrast to TOC, TN concentrations in the upper layer of water column are very low (5-30 μM) (Fig. 2 i & j). In the next section we show how the TOC affects the DO concentrations.

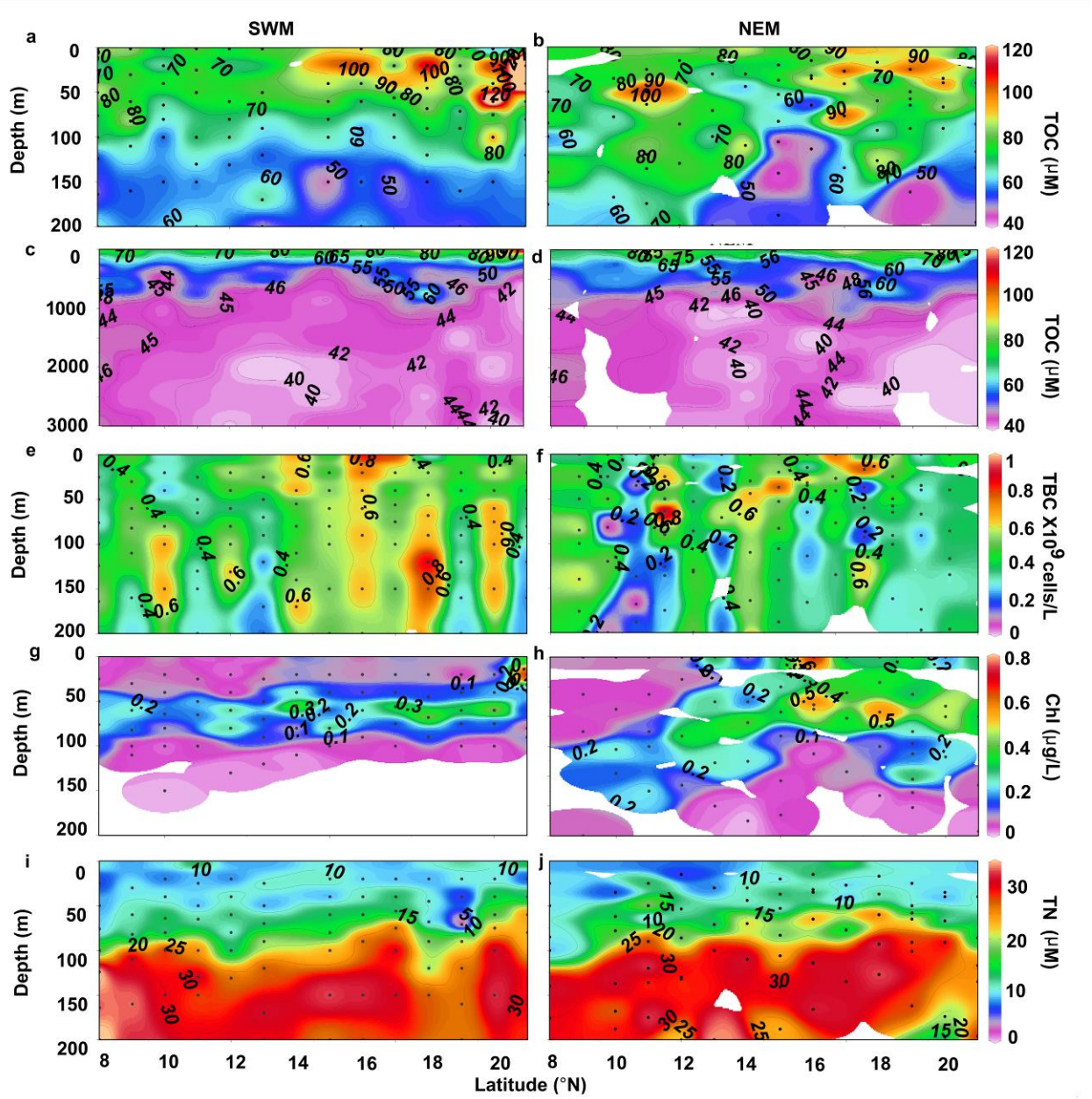

Figure 2: Latitudinal variation of TOC (upper 200m (a,b) and upto 3000m (c, d), TBC (e,f), Chl*a* (g,h) and TN (i,j) during SWM and NEM along 68°E transect.

3.2 Correlation between TOC and AOU

We used model (II) regression to evaluate the relationship between TOC and AOU. Earlier study by Doval and Hansell (2000) has suggested that the TOC and AOU relationship over entire depth underestimates the contribution of TOC oxidation to the development of AOU. The present study evaluated the TOC and AOU relationship along isopycnal surfaces. Potential density ($\sigma\theta$) is high in the northern AS wherein σ_θ > 23.5 kg/m^3 occur at the surface in stations north of 12°N and 9°N during NEM and SWM respectively (Fig 3 a & b). While the $\sigma\theta$ of 24.5 kg/m^3 lie between 40 and 50

m in the northern stations, it was at >100 m in few southern stations during both NEM and SWM (Fig 3a & b). The contribution of TOC to oxygen consumption along isopycnal surfaces was determined after converting AOU to carbon equivalents. TOC/AOU-C represents the contribution of TOC to AOU and is calculated with AOU in equivalents, using a Redfield ratio $-\Delta C/\Delta O_2 = 0.72$ (Anderson, 1995). The TOC/AOU-C, in equivalent carbon units, was maximum for the $\sigma\theta$ between 24.5 and 27.3 kg/m^3 and ranged from 14.3% during NEM to 22.5% during SWM (Table 2 and Fig 3 c & d). Surface waters showed minor TOC/AOU-C ranging from 9.2% during NEM to 11.1% during SWM. At deeper depths ($\sigma\theta$ > 27.3 kg/m^3) the TOC/AOU-C was minimal (Table 1).

Table 2: Slope Model II between TOC (µmol/kg) and AOU (µmol/kg).

Season	σ_θ kg/m^3	8°N to 21°N Depth (m)	TOC/AOU (molar ratio)	TOC/AOU-C (%)	r^2	n
NEM	<24.5	<122 m	-0.066 (±0.058)	9.2	0.03	45
SWM	<24.5	<112 m	-0.08 (± 0.055)	11.1	0.04	50
NEM	24.5 to 27.3	45 m to 725 m	-0.1027(±0.034)	14.3	0.13	60
SWM	24.5 to 27.3	48 m to 732 m	-0.162 (± 0.023)	22.5	0.41	71
NEM	>27.3	>725m to 3000m	-0.017(± 0.016)	2.4	0.03	40
SWM	>27.3	>732 m to 3000m	+0.005 (±0.006)	-	0.008	63

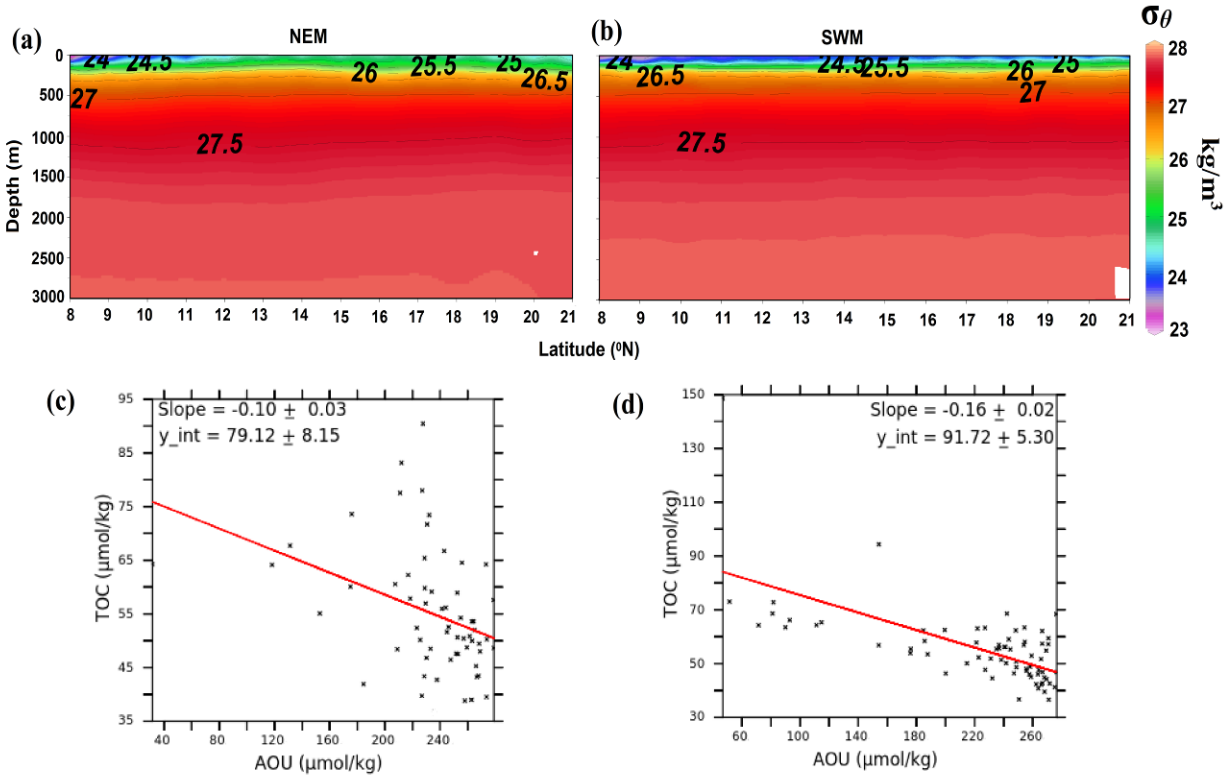

Figure 3: Potential density ($\sigma\theta$) during (a) NEM and (b) SWM along 68°E transect. Regression of TOC on AOU along the isopycnal layers 24.5–27σ_θ plotted using model II linear

Discussion

Small changes in the organic carbon (OC) pool could have important consequences towards the atmospheric CO_2 and thus climate (Castillo et al., 2016). Climate change and eutrophication are expected to drive significant decrease in the O_2 levels in the global ocean over the next few decades (Bopp et al., 2013; Cocco et al., 2013). The warming is already causing expansion and intensification of oceanic perennial OMZs (Stramma et al., 2008; Deutsch et al., 2011). OC can have a strong bearing on the intensification of OMZ, therefore, in this study we focus on the seasonal and spatial variability of OC in the AS and its comparison with the past data.

4.1 Seasonal variability of TOC

The spatial distribution of TOC suggests a significant north-south variation with higher concentrations towards the north (Fig. 2a & b). TOC concentrations were high during the SWM, especially in the surface layers which can be attributed to shallow mixed layer depth (MLD) as fresh TOC can be held near the surface (Sohrin and Semper 2005). Elevated TOC may be derived mostly from terrestrial inputs or from in situ production (Ribas et al., 2011). Recently, Al-Said et al. (2018) showed high concentration of TOC in the Gulf region and suggested that this high TOC could be exported to the northwest Indian Ocean along with the high saline PGW. We also observed a strong south-eastward current towards the northern stations. These currents might have exported high TOC from the Gulf regions in to the northern stations during recent years (Fig. 1a). The low TOC during NEM could be attributed to the deeper mixed layer than the euphotic zone that suppresses primary production despite available nutrients (Naqvi et al., 2002). Also NEM is known to have high bacterial abundance (Jain et al., 2014), which would control the rise in OC (Ribas et al., 2011). Earlier Sardessai et al. (1998) reported that the POC concentrations were lower during NEM, and the concentration increases towards the north. The comparison between Chl*a* and TOC shows that most of the TOC during SWM is not locally produced, while during NEM it is mainly produced by photosynthesis in the euphotic zone (Fig.2). TOC at deeper depths was constant and didn't show any seasonality, which implies that organic carbon in the deep water is biochemically inert.

4.2 Oxygen consumption by TOC

The oceanic oxygen levels are maintained by the balance between supply and consumption. Supply is through exchange with the atmosphere and thermohaline circulations while consumption is mainly by organic matter respiration. AOU in the ocean depends not only on respiration but is strongly influenced by transport processes and eventually lost at the ocean surface (Koeve and Kahler 2016). The TOC/AOU-C have a large range, from ~20% in the equatorial regions to ~80% in subtropical

gyres (Pan et al., 2014). In the present study, TOC was inversely correlated with AOU during both the seasons (Fig. 3 c,d). The TOC/AOU-C was calculated by using the slope of the model II linear regression between TOC and AOU for isopycnal surfaces (Table 2) following Doval and Hansell (2000). TOC oxidation was responsible for 14.3% and 22.5% of oxygen consumption during NEM and SWM, respectively for $\sigma\theta$ between 24.5 to 27.3 kg/m^3. These levels are close to the range to those reported earlier (18 - 43%) in the upper Indian Ocean by Doval and Hansell (2000). Although, Doval and Hansell (2000) reported such values for the $\sigma\theta$ between 23 and 27 kg/m^3, the depth ranges were similar. Earlier Kumar et al. (1990) had given TOC/AOU-C for entire water column in the north western Indian Ocean (slope=-0.062, which is ~8.6%).

4.3 Comparison of recent data with US-JGOFS

In addition to the seasonal variability of TOC, we also compared the TOC variation during the US-JGOFS with the present time. TOC's vertical profiles at ASTS (recent data) and at N9 during US-JGOFS clearly showed higher TOC during recent years for all 3 seasons (NEM, SWM and spring intermonsoon; SIM) with a difference of 10 to 20µM in the surface waters (Fig. 4). TOC decreased with depth and was about half of the surface concentrations below 800m. TOC concentrations were nearly constant at depths below ~1000m. POC also showed a similar trend to TOC; however, POC changes were more prominent than TOC. Surface water POC, which was <5 µM until 2011, doubled by 2017. POC reached a maximum concentration of 14 µM. This rise in POC in recent years is important as the POC reported in the mixed layer of the AS is known to be <5 µM (Hansell and Peltzer et al., 1998). The excess POC in the mixed layer would be sinking to deeper layers and would lead to oxygen consumption.

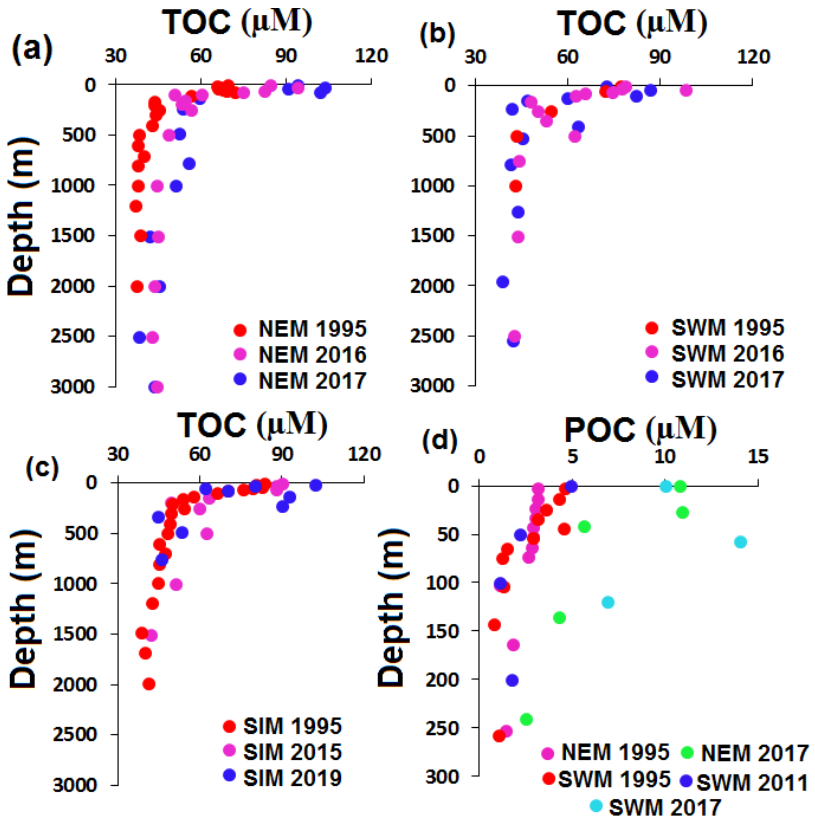

Figure 4: Vertical distribution of TOC (µM) at the ASTS station (recent data) and at station N9 of US-JGOFS during (a) NEM, (b) SWM, (c) SIM. (d)Vertical distribution of POC during SWM and NEM with a comparison with US-JGOFS data.

To understand the role of water masses towards the TOC variability, we have identified the relevant water masses in the study area. The important water masses are ASHSW, PGW and RSW (Morrison, 1997). Figure 5 shows the seasonal variation of TOC concentrations during US- JGOFS and recent time. It clearly indicates that the TOC concentration has increased during the recent time especially in the ASHSW. The mean concentration of TOC in different water masses is calculated for US-JGOFS and present study, by using the water mass criteria mentioned in table 1. The mean TOC in the ASHSW during SWM in the present study is 81.8±17µM, whereas

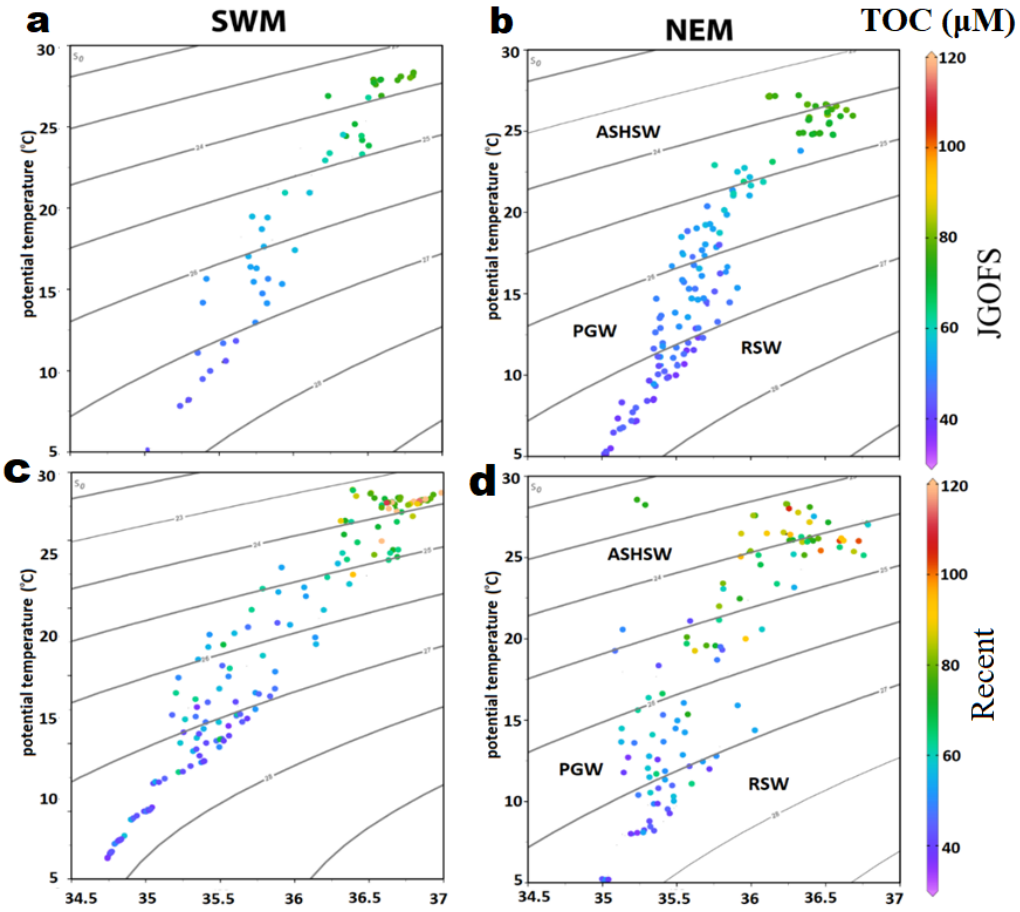

Figure 5: Seasonal variations of TOC in the AS plotted on TS diagrams along the (a,b) US-JGOFS transect of 1995 and (c,d) recent data.

during JGOFS it was 73.9±3.4 µM. In the PGW the mean TOC during SWM was 52.8±6.6 µM and 51.7±1.5 µM during present study and JGOFS, respectively. In the Red Sea water mass the mean TOC was 47.8±7.9 µM and 45.3±5.5 µM during present study and JGOFS, respectively. Similar to SWM, the NEM also showed higher values during recent years. The mean TOC in the ASHSW was 79.3±11 µM and 75.6±4.7 µM during present study and JGOFS, respectively. In the PGW the mean TOC during SWM was 50 ±7 µM and 49±3.4 µM during present study and JGOFS, respectively. In the Red Sea water mass the mean TOC was 47.6±5.8 µM and 43.7±4 µM during present study and JGOFS, respectively. Though the TOC values during recent observation was higher than US-JGOFS in all the water masses, ASHSW showed maximum variation during both seasons. Also, as seen from the rise in POC concentrations in recent years, the observed rise in TOC could be contributed by POC instead of DOC.

Figures 6 and 7 show a comparison of the vertical distribution of temperature, salinity, DO, TOC and Chl*a* during SWM and NEM of US JGOFS with recent data. During SWM, temperature in the upper layer slightly increased in the recent year (2016) along with maximum warming in the southern region (Fig. 6a & b), while salinity showed higher values in the northern stations during the recent year (Fig. 6c & d) along with shoaling of 4 ml/L DO (Fig 6e & f). However, TOC showed significant increase during the recent year with maximum concentration in the northern region (Fig.6g &h). In contrast to TOC, subsurface Chl*a* showed lower concentration during the recent year compared to JGOFS (Fig. 6 i & j).

During the NEM, temperature showed significant increase in the recent year (2017) with maximum warming in the southern region (Fig. 7a &b). Salinity also showed higher (~0.25) values during recent years (Fig. 7c & d). Similar to SWM, shoaling of 2.5ml/L DO is observed during the recent NEM (Fig. 7e & f).These figures clearly show that the temperature and TOC in the top 100 m have increased in the recent years along with a decrease in oxygen and Chl*a* levels. Besides, the salinity distributions show more intrusion of ASHSW during the recent years (especially during the SWM) compared to 1995.

We also analyzed the temporal anomalies of temperature (Fig. 8a) and salinity (Fig. 8b) at ASTS (17^{o}N-21^{o}N & 60^{o}E-70^{o}E averaged) in the upper 200 m from 1994 to 2017. This analysis clearly shows an increase in temperature and salinity of the ASHSW from 2014 to 2017. Similar findings were also reported by Zhang et al. (2020), clearly showing positive salinity anomalies during 2014–17 with the regional mean value increased by more than 0.14 at its peak.

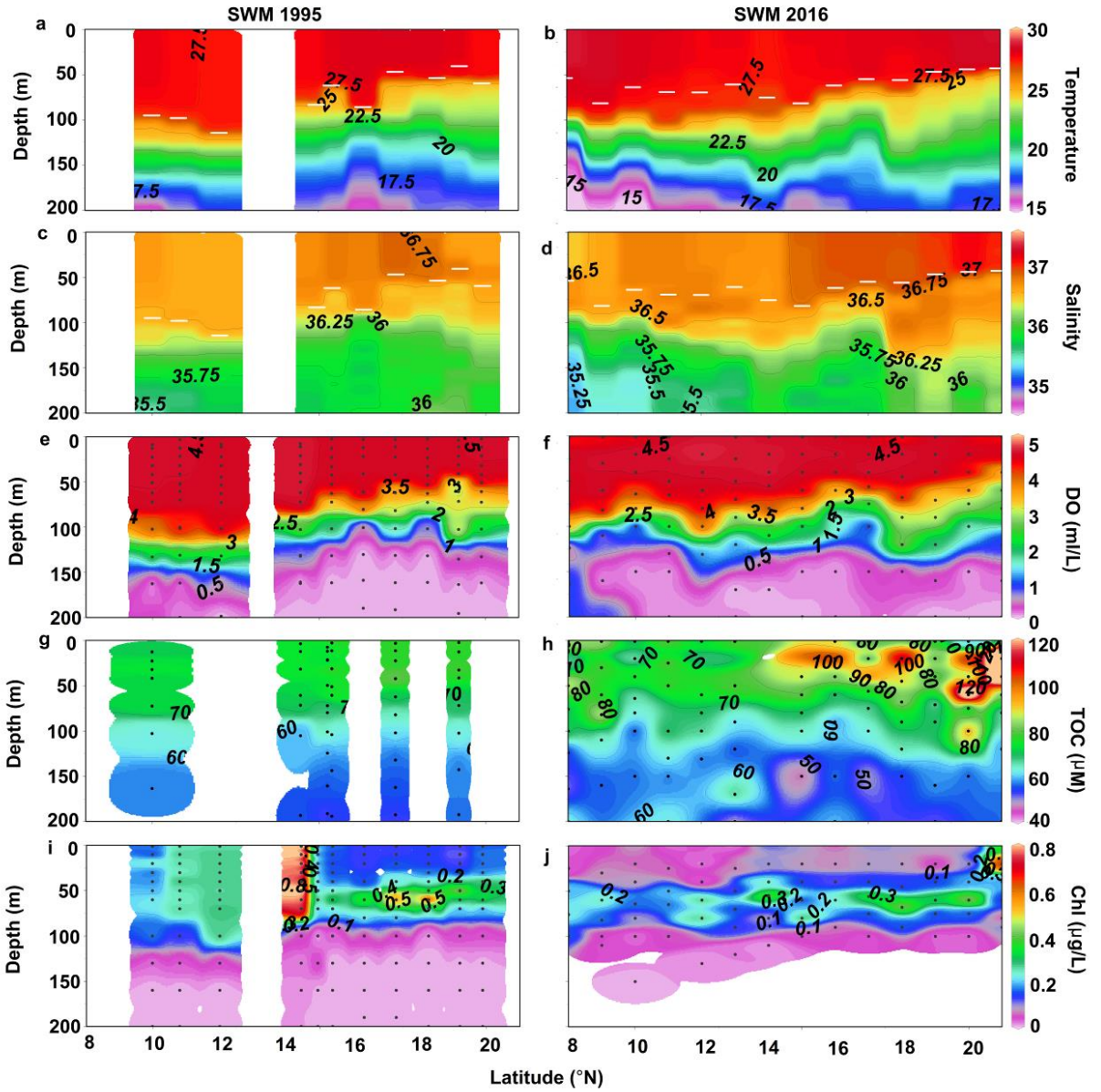

Figure 6: Vertical distribution of temperature, salinity, DO, TOC, and Chl*a* during SWM of US-JGOFS transect (1995) and 2016 (recent). The white dashed lines in temperature and salinity figures indicate the MLD.

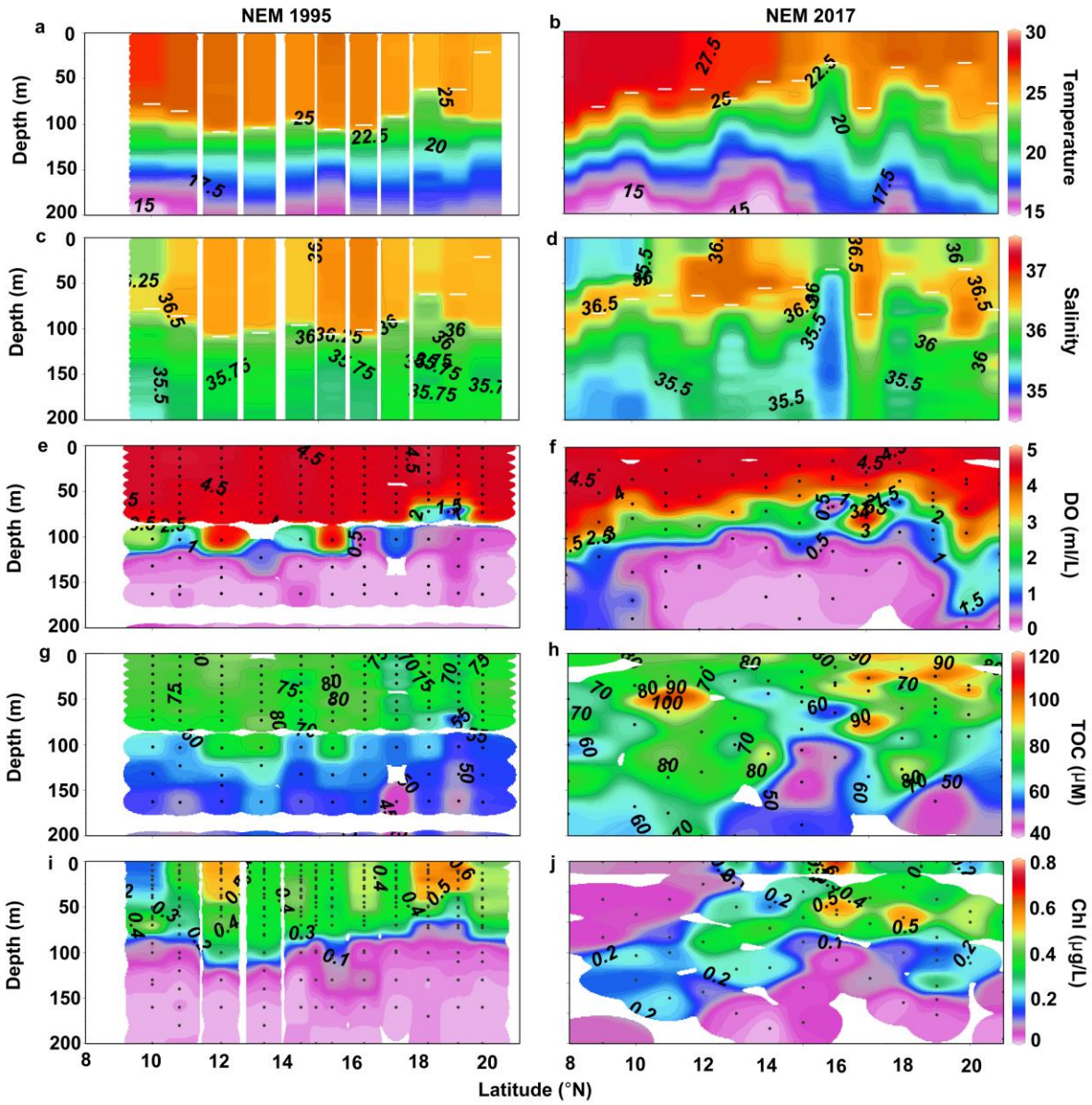

Figure 7: Vertical distribution of temperature, salinity, DO, TOC and Chl*a* during NEM of US-JGOFS transect (1995) and 2017 (recent). The white dashed lines in temperature and salinity figures indicate the MLD.

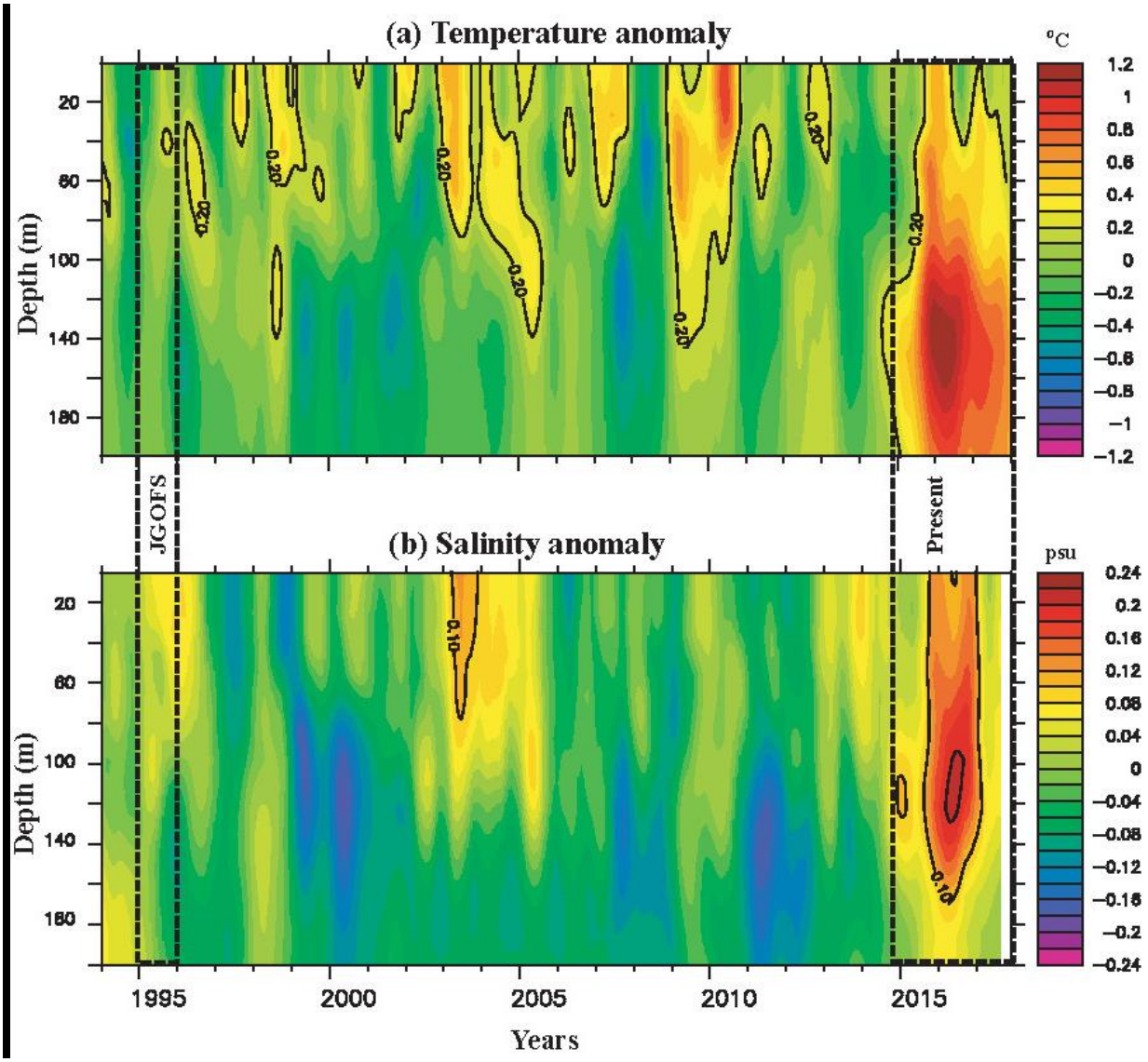

Figure 8: Temporal anomalies of temperature and salinity at ASTS (17°N-21°N & 60°E-70°E averaged) in the upper 200 m during 1994 to 2017.

4.4 Implication of present study

Ocean deoxygenation has been mainly attributed to low solubility of DO at higher temperatures, increased stratification that reduces the ventilation and higher respiration rates in warmer waters. The present study highlights warmer temperatures and low Chl*a* in recent years (Figs. 6 & 7) in comparison to US-JGOFS data. Earlier Banse et al. (2014) also reported higher depletion of DO during NEM. Apart from the well-studied causes for deoxygenation, here we try to explore other plausible reasons that could deoxygenate the AS. Figure 4 shows the rise in POC in recent years, that would be vertically exported to the subsurface layers and consume DO. Figures 6 and 7 clearly show that the TOC has also increased in the recent years despite a drop in the Chl*a* levels indicating other than biological sources for TOC. Earlier, Menzel (1964) also observed that OC in seawater is not

rapidly influenced by biological activity and is not directly related to primary production but more to do with the hydrodynamic processes.

Despite the drop in Chl *a*, the TBC obtained in the present study was high during both SWM and NEM as compared to the Indian JGOFS data (Ramaiah et al., 1996). They reported TBC counts of $0.5x10^9$/L during SWM and $<0.1x10^9$/L during NEM. This finding suggests that despite the drop in primary productivity, the bacterial carbon demand is met and infact they are flourished, indicating an alternate source of carbon. Earlier studies by Naqvi & Shailaja (1993) and Ducklow (1993) suggested that the sinking flux of POC was inadequate to sustain the respiration rates in the AS. Subsequently, Naqvi et al. (2006) suggested that additional supply of organic matter to the OMZ could be either quasi-horizontally or from the continental margins. Recently, Sharples et al. (2017) showed that low-latitude shelf seas are significant exporters of allochthonous organic matter due to weak Coriolis-driven circulation and greater TOC loading from tropical rivers. The PGW is associated with substantially higher TOC (8–12 μM), than the water it mixes within the Sea of Oman and the AS (Hansell and Peltzer, 1998). Recently, Al-Said et al. (2018) reported that the high-salinity water mass that flows out of the Gulf has high concentrations of TOC and may cause expansion/intensification of the AS OMZ.

Based on Al-Said et al. (2018) report, we have looked into the different water masses that move from the northern AS to the south. The ASHSW is formed during winter by atmospheric forcing, a combination of both heat and freshwater fluxes. Its southward extension is limited by north equatorial current during winter and Indian monsoon current during summer (Prasanna Kumar and Prasad 1999). Figures 6c & d clearly shows that the southern extent of the ASHSW has increased during SWM, indicating that the Indian monsoon current has weakened due to recent warming in the AS. Observational analysis by Sun et al. (2019) suggests that the warming rate of the AS has significantly increased during the past two decades. D mello and Prasanna Kumar (2018) related the increase in warming to changes in rates of evaporation. Roxy et al. (2014) showed that the western tropical Indian Ocean is warming faster than the rest of the tropical oceans, while Dinesh Kumar et al. (2016) reported an increasing SST of 0.12°C per decade in the AS for the period from 1960 to 2009.

Dinesh Kumar et al. (2016) also reported decreasing surface wind speed trends, latent heat flux, and the advective process *via* the weakened surface currents. Recently, Swapna et al. (2017) indicated a weakening of the Indian summer monsoon circulation in the last few decades, accompanied by reduced upwelling off Arabia and Somalia. Parvathi et al. (2017) indicate warming driven reduction in winter convective mixing in the AS. Although wind speed over the last 20 years did not show a

significant change (Fig. S2), our recent observation during SWM showed an intensification of the south-westward current (Fig.1a) which allow the transport of more ASHSW to the northwest Indian Ocean favoring additional transport of high TOC to the eastern AS. This was supported by Zhang et al. (2020) who clearly showed positive salinity anomalies in the AS with the regional mean value increased by more than 0.14 at its peak during 2014–17. They identified, a prolonged high-salinity event during 2014–17, when both the volumes of the surface ASHSW and the intermediate PGW increased, with the volume of the low salinity water between them reduced. Although we did not observe significant anomaly in the PGW (not shown), the salinity anomaly was strong in the ASHSW (Fig 8b), which could be related to higher TOC in the ASHSW than in the PGW (Fig. 5). Hence our results highlight the role of transport processes in supplying high TOC in the northeastern AS during recent years.

Other possible sources of TOC into the AS could be from atmospheric deposition or from lateral advection. Recently, Mao et al. (2014) reported that the mean aerosol optical depth (AOD) over the Indian Ocean has increased in the last ten years. This indicates that we cannot rule out the possibility of TOC source from the atmosphere; however, to our knowledge, there are no direct measurements of TOC coming into the AS through the aerosols. Apart from input from aerosols, the warming driven changes in bacterial productivity and zooplankton grazing can also add TOC into the AS.

The observed warming will decrease the DO solubility, but the drop in Chl*a* would reduce the oxygen demand in the OMZ. However, excess POC might result in consumption of oxygen and further contribute to the expansion of the OMZ. Considering that a 10μM increase in the labile/semi-labile fraction of TOC in the PGW could lead to 2.6–8% increase in nitrogen loss through denitrification (Al-Said et al., 2018), the high TOC observed during recent times draws scientific attention. This higher TOC, in the form of POC into the AS will further expand and intensify the OMZ and contribute towards nitrogen loss.

Conclusions

TOC concentrations in the AS showed seasonal variations with high values during SWM as compared to NEM, with higher concentrations towards the northern stations. TOC oxidation contributed 14.3% and 22.5% of oxygen consumption during NEM and SWM in the σ_θ range from 24.5 to 27.3 kg/m^3. Based on in situ observations and comparison with previous data, the present study clearly shows a rise in temperature, POC and drop in Chl*a* in the last 2 decades. The ASHSW intrusion towards the south has increased and carries excess TOC into the AS especially during the SWM. This excess TOC supports high abundance of TBC in the eastern AS. Although the observed

warming is expected to decrease the DO solubility, while the drop in Chl*a* will reduce the oxygen demand in the OMZ, the excess POC might result in the consumption of oxygen and further contribute to the ongoing expansion of the AS OMZ. This study attains a great significance especially in modelling studies considering the missing links with respect to role of transport processes and biological oxygen demand in ocean deoxygenation.

Acknowledgement

We thank the Director, CSIR- NIO for his support and encouragement. We would like to thank the US- JGOFS team for granting permission to use JGOFS data. We greatly acknowledge the guidance received from Dr. S.W.A. Naqvi during this study. We are grateful to the chief scientists and scientific team onboard for their co-operation and support. AV. Chndrasekhararao is acknowledged for his assistance in HPLC analysis.. This study was carried out as a part of the projects PSC-0108 (INDIAS-IDEA) funded by CSIR, and GAP-2425 (SIBER-INDIA) funded by the Ministry of Earth Sciences, New Delhi. This is NIO contribution No: XXXX.

References

1. Al-Said T, Naqvi SW, Al-Yamani F, Goncharov A, Fernandes L. High total organic carbon in surface waters of the northern Arabian Gulf: Implications for the oxygen minimum zone of the Arabian Sea. Marine pollution bulletin. 2018 Apr 1;129(1):35-42.

2. Badr ES, Achterberg EP, Tappin AD, Hill SJ, Braungardt CB. Determination of dissolved organic nitrogen in natural waters using high-temperature catalytic oxidation. TrAC Trends in Analytical Chemistry. 2003 Dec 1;22(11):819-27.

3. Balmaseda M A, Mogensen K and Weaver A T, Evaluation of the ECMWF ocean reanalysis system ORAS4 Q. J. R. Meteorol. Soc. 2013, 139 1132–61.

4. Banse K. Seasonality of phytoplankton chlorophyll in the central and northern Arabian Sea. Deep Sea Research Part A. Oceanographic Research Papers. 1987 May 1;34(5-6):713-23.

5. Banse K, Naqvi SW, Narvekar PV, Postel JR, Jayakumar DA. Oxygen minimum zone of the open Arabian Sea: variability of oxygen and nitrite from daily to decadal timescales. Biogeosciences, 2014, 11, 2237–2261.
6. Beal LM, Ffield A, Gordon AL. Spreading of Red Sea overflow waters in the Indian Ocean. Journal of Geophysical Research: Oceans. 2000 Apr 15;105(C4):8549-64.

7. Benson, B.B., and Krauss, O. The concentration and isotopic fractionation of oxygen dissolved in freshwater and seawater in equilibrium with the atmosphere. Limnology Oceanography, 1984. 10, 264-277.

8. Blake ES, Landsea C, Gibney EJ. The deadliest, costliest, and most intense United States tropical cyclones from 1851 to 2010 (and other frequently requested hurricane facts) 2011.Bopp L, Resplandy L, Orr JC, Doney SC, Dunne JP, Gehlen M, Halloran P, Heinze C, Ilyina T, Seferian R, Tjiputra J. Multiple stressors of ocean ecosystems in the 21st century: projections with CMIP5 models. Biogeosciences. 2013 Oct 2;10:6225-45.
9. Breitburg D, Levin LA, Oschlies A, Grégoire M, Chavez FP, Conley DJ, Garçon V, Gilbert D, Gutiérrez D, Isensee K, Jacinto GS. Declining oxygen in the global ocean and coastal waters. Science. 2018 Jan 5;359(6371):eaam7240.

10. Carpenter JH. The Chesapeake Bay Institute technique for the Winkler dissolved oxygen method. Limnology and Oceanography. 1965 Apr;10(1):141-3.

11. Carpenter, J.H., 1965. The Chesapeake Bay Institute technique for the Winkler dissolved oxygen method. Limnology Oceanography 10, 141–143.
12. Chndrasekhararao AV, Kurian S, Vidya PJ, Gauns M, Shenoy DM, Mulla A, Naik H, Reddy TV, Naqvi SW. Phytoplankton response to the contrasting physical regimes in the eastern Arabian Sea during north east monsoon. Journal of Marine Systems. 2018 Jun 1;182:56-66.
13. Cocco V, Joos F, Steinacher M, Frölicher TL, Bopp L, Dunne J, Gehlen M, Heinze C, Orr J, Oschlies A, Schneider B. Oxygen and indicators of stress for marine life in multi-model global warming projections. Biogeosciences. 2013;10(3):1849-68.
14. Codispoti LA, Brandes JA, Christensen JP, Devol AH, Naqvi SW, Paerl HW, Yoshinari T. The oceanic fixed nitrogen and nitrous oxide budgets: Moving targets as we enter the anthropocene?. Scientia Marina. 2001 Dec 30;65(S2):85-105.
15. Codispoti LA. Interesting times for marine N2O. Science. 2010 Mar 12;327(5971):1339-40.

16. Dai M, Meng F, Tang T, Kao SJ, Lin J, Chen J, Huang JC, Tian J, Gan J, Yang S. Excess total organic carbon in the intermediate water of the South China Sea and its export to the North Pacific. Geochemistry, Geophysics, Geosystems. 2009 Dec;10(12).

17. De Sousa SN, Kumar MD, Sardessai S, Sarma VV. Seasonal variability in oxygen and nutrients in. Current science. 1996 Dec 10;71(11).

18. Deutsch C, Brix H, Ito T, Frenzel H, Thompson L. Climate-forced variability of ocean hypoxia. science. 2011 Jul 15;333(6040):336-9.
19. Dickey T, Marra J, Sigurdson DE, Weller RA, Kinkade CS, Zedler SE, Wiggert JD, Langdon C. Seasonal variability of bio-optical and physical properties in the Arabian Sea: October 1994-October 1995. Deep-sea research. Part II, Topical studies in oceanography. 1998 Aug 1;45(10-11):2001-25.

20. Dickson AG, Sabine CL, Christian JR. Guide to best practices for ocean CO_2 measurements. North Pacific Marine Science Organization; 2007.

21. D'Mello JR, Prasanna Kumar S. Processes controlling the accelerated warming of the Arabian Sea. International Journal of Climatology. 2018 Feb;38(2):1074-86.
22. Doval MD, Hansell DA. Organic carbon and apparent oxygen utilization in the western South Pacific and the central Indian Oceans. Marine Chemistry. 2000 Jan 1;68(3):249-64.
23. Ducklow HW. Bacterioplankton distributions and production in the northwestern Indian Ocean and Gulf of Oman, September 1986. Deep Sea Research Part II: Topical Studies in Oceanography. 1993 Jan 1;40(3):753-71.
24. Dueser WG, Ross EH, Mlodzinska ZJ. Evidence for and rate of denitrification in the Arabian Sea. Deep Sea Research. 1978 May 1;25(5):431-45.

25. Findlater J. A major low-level air current near the Indian Ocean during the northern summer. Quarterly Journal of the Royal Meteorological Society. 1969 Apr;95(404):362-80.

26. Garcia, H.E. and Gordon, L.I.. Oxygen solubility in seawater: Better fitting equations. Limnology Oceanography. 1992, 37, 1307-1312.

27. Grasshoff P. Methods of seawater analysis. Verlag Chemie. FRG. 1983;419:61-72.
28. Hansell DA, Peltzer ET. Spatial and temporal variations of total organic carbon in the Arabian Sea. Deep Sea Research Part II: Topical Studies in Oceanography. 1998 Aug 1;45(10-11):2171-93.
29. Heukelem, Van, 2002. HPLC phytoplankton pigments: Sampling, laboratory methods, andquality assurance procedures. In: Mueller, J., Fargion, G. (Eds.), Ocean OpticsProtocols for Satellite Ocean Color Sensor, Revision 3, Volume 2, Chapter 16, NASA Technical Memorandum 2002–2004, pp. 258–268.
30. Jain A, Bandekar M, Gomes J, Shenoy D, Meena RM, Naik H, Khandeparkar R, Ramaiah N. Temporally invariable bacterial community structure in the Arabian Sea oxygen minimum zone. Aquatic Microbial Ecology. 2014 Aug 29;73(1):51-67.
31. Joseph S, Freeland HJ. Salinity variability in the Arabian Sea. Geophysical research letters. 2005 May;32(9).
32. Karstensen J, Stramma L, Visbeck M. Oxygen minimum zones in the eastern tropical Atlantic and Pacific oceans. Progress in Oceanography. 2008 Jun 1;77(4):331-50.
33. Keeling RF, Körtzinger A, Gruber N. Ocean deoxygenation in a warming world. Annual review of marine science. 2010 Jan 15;2:199-229.

34. Koeve W, Kähler P. Oxygen utilization rate (OUR) underestimates ocean respiration: A model study. Global Biogeochemical Cycles. 2016 Aug;30(8):1166-82.
35. Kumar MD, Rajendran A, Somasundar K, Haake B, Jenisch A, Shuo Z, Ittekkot V, Desai BN. Dynamics of dissolved organic carbon in the northwestern Indian Ocean. Marine Chemistry. 1990 Dec 10;31(1-3):299-316.
36. Kumar PD, Paul YS, Muraleedharan KR, Murty VS, Preenu PN. Comparison of long-term variability of Sea Surface Temperature in the Arabian Sea and Bay of Bengal. Regional Studies in Marine Science. 2016 Jan 1;3:67-75.
37. Kumar SP, Prasad TG. Winter cooling in the northern Arabian Sea. Current Science. 1996 Dec 10:834-41.
38. Kumar SP, Prasad TG. Formation and spreading of Arabian Sea high-salinity water mass. Journal of Geophysical Research: Oceans. 1999 Jan 15;104(C1):1455-64.
39. Kurian S, Roy R, Repeta DJ, Gauns M, Shenoy DM, Suresh T, Sarkar A, Narvenkar G, Johnson CG, Naqvi SW. Seasonal occurrence of anoxygenic photosynthesis in Tillari and Selaulim reservoirs, Western India. Biogeosciences Discussions. 2011 Nov 1;8(6).
40. Lachkar Z, Lévy M, Smith KS. Strong intensification of the Arabian Sea oxygen minimum zone in response to Arabian Gulf warming. Geophysical Research Letters. 2019 May 28;46(10):5420-9.
41. Lam P, Kuypers MM. Microbial nitrogen cycling processes in oxygen minimum zones. Annual review of marine science. 2011 Jan 15;3:317-45.
42. Letscher RT, Hansell DA, Carlson CA, Lumpkin R, Knapp AN. Dissolved organic nitrogen in the global surface ocean: Distribution and fate. Global Biogeochemical Cycles. 2013 Mar;27(1):141-53.
43. Madhupratap M, Kumar SP, Bhattathiri PM, Kumar MD, Raghukumar S, Nair KK, Ramaiah N. Mechanism of the biological response to winter cooling in the northeastern Arabian Sea. Nature. 1996 Dec;384(6609):549-52.
44. Mao KB, Ma Y, Xia L, Chen WY, Shen XY, He TJ, Xu TR. Global aerosol change in the last decade: An analysis based on MODIS data. Atmospheric Environment. 2014 Sep 1;94:680-6.
45. Menzel DW. The distribution of dissolved organic carbon in the Western Indian Ocean. InDeep Sea Research and Oceanographic Abstracts 1964 Oct 1 (Vol. 11, No. 5, pp. 757-765). Elsevier.
46. Morrison JM. Inter-monsoonal changes in the T-S properties of the near-surface waters of the northern Arabian Sea. Geophysical Research Letters. 1997 Nov 1;24(21):2553-6. Naqvi SW, Naik H, Jayakumar DA, Shailaja MS, Narvekar PV. Seasonal oxygen deficiency over the western continental shelf of India. InPast and Present water column anoxia 2006 (pp. 195-224). Springer, Dordrecht.
47. Naqvi SW, Sarma VV, Jayakumar DA. Carbon cycling in the northern Arabian Sea during the northeast monsoon: Significance of salps. Marine Ecology Progress Series. 2002 Jan 31;226:35-44.
48. Naqvi SW, Shailaja MS. Activity of the respiratory electron transport system and respiration rates within the oxygen minimum layer of the Arabian Sea. Deep Sea Research Part II: Topical Studies in Oceanography. 1993 Jan 1;40(3):687-95.
49. Naqvi SW. Some aspects of the oxygen-deficient conditions and denitrification in the Arabian Sea. Journal of Marine Research. 1987 Nov 1;45(4):1049-72.
50. Oschlies A, Brandt P, Stramma L, Schmidtko S. Drivers and mechanisms of ocean deoxygenation. Nature Geoscience. 2018 Jul;11(7):467-73.

51. Pan X, Achterberg EP, Sanders R, Poulton AJ, Oliver KI, Robinson C. Dissolved organic carbon and apparent oxygen utilization in the Atlantic Ocean. Deep Sea Research Part I: Oceanographic Research Papers. 2014 Mar 1;85:80-7.
52. Panagiotopoulos, C., Pujo-Pay, M., Benavides, M., Van Wambeke, F., and Sempéré, R.: The composition and distribution of semi-labile dissolved organic matter across the southwest Pacific, Biogeosciences, 2019; 16: 105–116.

53. Parsons TR, Maita Y, Lalli CM. A manual of chemical and biological methods for seawater analysis. Pergamon, Oxford sized algae and natural seston size fractions. Marine Ecology Progress Series. 1984;199:43-53.

54. Parvathi V, Suresh I, Lengaigne M, Izumo T, Vialard J. Robust projected weakening of winter monsoon winds over the Arabian Sea under climate change. Geophysical Research Letters. 2017 Oct 16;44(19):9833-43.

55. Pearson. On lines and planes of closest fit to systems of points in space. Phil. Mag. 1901, 6: 559-572.

56. Prasad, T.G., Ikeda, M. and Kumar, S.P., 2001. Seasonal spreading of the Persian Gulf Water mass in the Arabian Sea. Journal of Geophysical Research: Oceans, 106(C8), 17059-17071.

57. Ramaiah N, Raghukumar S, Gauns M. Bacterial abundance and production in the central and eastern Arabian Sea. Current Science. 1996 Dec 10:878-82.

58. Ribas-Ribas M, Gómez-Parra A, Forja JM. Spatio-temporal variability of the dissolved organic carbon and nitrogen in a coastal area affected by river input: The north eastern shelf of the Gulf of Cádiz (SW Iberian Peninsula). Marine Chemistry. 2011 Sep 20;126 (1-4):295-308.
59. Rochford DJ. Salinity maxima in the upper 1000 metres of the north Indian Ocean. Marine and Freshwater Research. 1964; 15(1):1-24.
60. Romera-Castillo C, Letscher RT, Hansell DA. New nutrients exert fundamental control on dissolved organic carbon accumulation in the surface Atlantic Ocean. Proceedings of the National Academy of Sciences. 2016 Sep 20;113(38):10497-502.
61. Roshan S, DeVries T. Efficient dissolved organic carbon production and export in the oligotrophic ocean. Nature communications. 2017 Dec 11;8(1):1-8.
62. Roxy MK, Modi A, Murtugudde R, Valsala V, Panickal S, Prasanna Kumar S, Ravichandran M, Vichi M, Lévy M. A reduction in marine primary productivity driven by rapid warming over the tropical Indian Ocean. Geophysical Research Letters. 2016 Jan 28;43(2):826-33.
63. Roxy MK, Ritika K, Terray P, Masson S. The curious case of Indian Ocean warming. Journal of Climate. 2014 Nov;27(22):8501-9.
64. Sardessai S, Sarma VV, Kumar MD. Particulate organic carbon and particulate humic material in the Arabian Sea. . Indian Journal of Marine Sciences. 1999; 28: 5–9.
65. Schmidtko et al., 2017Schmidtko S, Stramma L, Visbeck M. Decline in global oceanic oxygen content during the past five decades. Nature. 2017 Feb;542(7641):335.
66. Sharples J, Middelburg JJ, Fennel K, Jickells TD. What proportion of riverine nutrients reaches the open ocean?. Global Biogeochemical Cycles. 2017 Jan 1;31(1):39-58.
67. Shenoy DM, Suresh I, Uskaikar H, Kurian S, Vidya PJ, Shirodkar G, Gauns MU, Naqvi SW. Variability of dissolved oxygen in the Arabian Sea Oxygen Minimum Zone and its driving mechanisms. Journal of Marine Systems. 2020 Jan 13:103310.
68. Shetye SS, Kurian S, Gauns M, Vidya PJ. 2015–16 ENSO contributed reduction in oil sardines along the Kerala coast, south-west India. Marine Ecology. 2019b Dec;40(6):e12568.

69. Shetye SS, Kurian S, Naik H, Gauns M, Chndrasekhararao AV, Kumar A, Naik B. Variability of organic nitrogen and its role in regulating phytoplankton in the eastern Arabian Sea. Marine pollution bulletin. 2019a Apr 1;141:550-60.
70. Stramma L, Johnson GC, Sprintall J, Mohrholz V. Expanding oxygen-minimum zones in the tropical oceans. Science. 2008 May 2;320(5876):655-8.
71. Sun C, Li J, Kucharski F, Kang IS, Jin FF, Wang K, Wang C, Ding R, Xie F. Recent acceleration of Arabian Sea warming induced by the Atlantic-western Pacific trans-basin multidecadal variability. Geophysical Research Letters. 2019 Feb 16;46(3):1662-71.
72. Swapna P, Jyoti J, Krishnan R, Sandeep N, Griffies SM. Multidecadal weakening of Indian summer monsoon circulation induces an increasing northern Indian Ocean sea level. Geophysical Research Letters. 2017 Oct 28;44(20):10-560.
73. Ward BB, Devol AH, Rich JJ, Chang BX, Bulow SE, Naik H, Pratihary A, Jayakumar A. Denitrification as the dominant nitrogen loss process in the Arabian Sea. Nature. 2009 Sep;461(7260):78.

74. Wyrtki K. Oceanographic atlas of the international Indian Ocean expedition. National Science Foundation; 1971.

75. York Least-squares fitting of a straight line. Canadian Journal of Physics. 1966. 44, 1079-1086.

76. Zhang Y, Yan DU, Jayarathna D, Qiwei SU, Yao F, Feng M. A prolonged high-salinity event in the Northern Arabian Sea during 2014-2017. Journal of Physical Oceanography. 2020*;* 50: 849–865..0

Online data

1. Azam, Farooq and Smith, David. “Particulate organic carbon” United States JGOFS Data Server. Woods Hole Oceanographic Institution, USA: U.S. JGOFS Data Management Office, iPub: 3 April 1998. http://usjgofs.whoi.edu/jg/serv/jgofs/arabian/ttn-043/poc_pon.html0

2. Bidigare Robert” HPLC_pigments” United States JGOFS Data Server. Woods Hole Oceanographic Institution, USA: U.S. JGOFS Data Management Office, iPub: 8 May 2001. http://usjgofs.whoi.edu/jg/serv/jgofs/arabian/ttn-050/HPLC_pigments.html0

3. Codispoti, Lou. “Hydrographic data” United States JGOFS Data Server. Woods Hole Oceanographic Institution, USA: U.S. JGOFS Data Management Office, iPub: 8 May 2000. http://usjgofs.whoi.edu/jg/serv/jgofs/arabian/ttn-043/bottle.html1

4. Codispoti, Lou. “Hydrographic data” United States JGOFS Data Server. Woods Hole Oceanographic Institution, USA: U.S. JGOFS Data Management Office, iPub: 8 May 2000. http://usjgofs.whoi.edu/jg/serv/jgofs/arabian/ttn-050/bottle.html0

5. Ducklow Hugh. “Particulate organic carbon” United States JGOFS Data Server. Woods Hole Oceanographic Institution, USA: U.S. JGOFS Data Management Office, iPub: 3 June, 1997. http://usjgofs.whoi.edu/jg/serv/jgofs/arabian/ttn-049/poc_pon.html0

6. Gardner, Wilford. ”Mixed layer” United States JGOFS Data Server. Woods Hole Oceanographic Institution, USA: U.S. JGOFS Data Management Office, iPub: 6 June 2002.

7. http://usjgofs.whoi.edu/jg/serv/jgofs/arabian/ttn-050/mixed_layer.html0

8. Gardner, Wilford. ”Mixed layer” United States JGOFS Data Server. Woods Hole Oceanographic Institution, USA: U.S. JGOFS Data Management Office, iPub: 6 June 2002.

9. http://usjgofs.whoi.edu/jg/serv/jgofs/arabian/ttn-043/mixed_layer.html0

10. Goericke, Ralf. ” HPLC_pigments” United States JGOFS Data Server. Woods Hole Oceanographic Institution, USA: U.S. JGOFS Data Management Office, iPub: 9 April 2002.http://usjgofs.whoi.edu/jg/serv/jgofs/arabian/ttn-043/HPLC_pigments.html0

11. Hansell, Dennis. “Total organic carbon” United States JGOFS Data Server. Woods Hole Oceanographic Institution, USA: U.S. JGOFS Data Management Office, iPub: 8 May, 2001. http://usjgofs.whoi.edu/jg/serv/jgofs/arabian/ttn-045/toc.html0

12. Hansell, Dennis. “Total organic carbon” United States JGOFS Data Server. Woods Hole Oceanographic Institution, USA: U.S. JGOFS Data Management Office, iPub: 9 September 1997. http://usjgofs.whoi.edu/jg/serv/jgofs/arabian/ttn-050/toc.html0

13. Morrison, John. “Ctd” United States JGOFS Data Server. Woods Hole Oceanographic Institution, USA: U.S. JGOFS Data Management Office, iPub: 5 November 1996. http://usjgofs.whoi.edu/jg/serv/jgofs/arabian/ttn-043/ctd.html0

14. Morrison, John. “Ctd” United States JGOFS Data Server. Woods Hole Oceanographic Institution, USA: U.S. JGOFS Data Management Office, iPub: 3 April, 1998. usjgofs.whoi.edu/jg/serv/jgofs/arabian/ttn-050/ctd.html0

15. Peltzer, E. “Total organic carbon” United States JGOFS Data Server. Woods Hole Oceanographic Institution, USA: U.S. JGOFS Data Management Office, iPub: 8 May, 2001. http://usjgofs.whoi.edu/jg/serv/jgofs/arabian/ttn-043/toc.html0.

Supplementary Fig 1: Latitudinal variation of DO during NEM (a) and SWM (b) at 68°E transect.

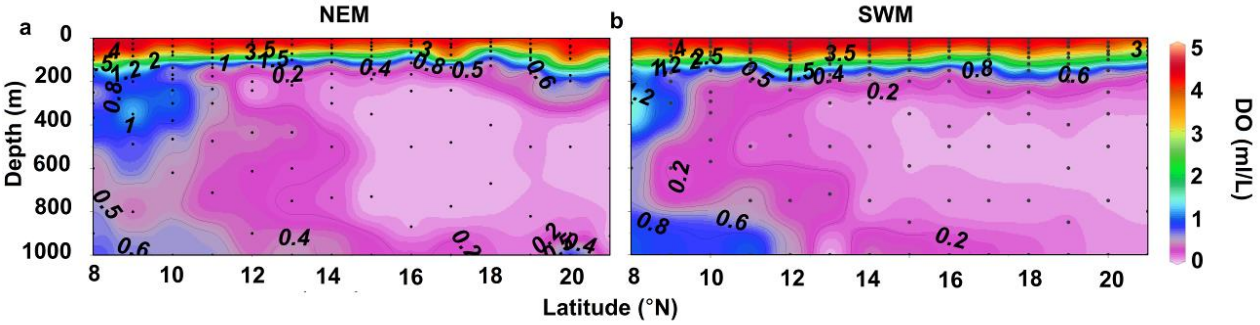

Supplementary Fig 2: Wind speed variations during SWM and NEM at ASTS from 1994 to 2019.